Ultracold ^{88}Sr atoms for an optical lattice clock

Thomas Legero, Joseph Sundar Raaj Vellore Winfred, Fritz Riehle, Uwe Sterr
Physikalisch-Technische Bundesanstalt
Braunschweig, Germany
Email: Thomas.Legero@ptb.de

***Abstract*— This paper reports results of cooling and trapping of ^{88}Sr for future use in an optical lattice clock. Strontium atoms are cooled to ultra-cold temperatures using a two-stage cooling process. In the first stage, atoms are captured from a Zeeman-slowed atomic beam and cooled to 2 mK in a magneto optical trap operated on the $^1S_0$ - $^1P_1$ transition at 461 nm. The second cooling stage utilizes the spin forbidden $^1S_0$ - $^3P_1$ transition at 689 nm. To reach ultra-cold temperatures, 50 ms of broadband cooling is followed by 28 ms long single frequency cooling. The transfer efficiency from the first to the second cooling stage was measured to be 23%, leaving 7×10^6 atoms at a temperature of 1 μK. The atomic cloud is overlapped with a horizontally oriented 1-D far-off resonance optical dipole trap (FORT) at 813 nm with an effective potential depth of 25 μK. Due to equal light shifts of the $^1S_0$ and the $^3P_1$ state simultaneous Doppler cooling during the atom loading into the FORT is possible which leads to a transfer efficiency into the dipole trap of up to 60 %**

I. Introduction

Since the first demonstration of a strontium optical lattice clock utilizing the light shift cancelation technique [1], the relative uncertainties of frequency measurements have approached the 10^{-15} level [2]–[5]. So far, mostly the fermionic isotope ^{87}Sr has been employed. However, the bosonic isotope ^{88}Sr offers the advantage of an improved signal-to-noise ratio and thus a higher stability due to its non-degenerate ground state and its high natural abundance. Several proposals have been made to extend the lattice clock scheme to ^{88}Sr [6]–[8]. Recently Baillard et al. evaluated the accuracy of an optical lattice clock with the bosonic isotope [9]. In contrast to ^{87}Sr where the clock transition is weakly allowed due to hyperfine mixing, the $^1S_0$ - $^3P_0$ transition in ^{88}Sr needs a supplementary coupling field, e.g. a dc-magnetic field can be used to enable this transition by field-induced state-mixing, which, on the other hand, leads to potentially large systematic shifts.

In this paper we report on the results of cooling ^{88}Sr down to temperatures below 1 μK using a two stage magneto-optical trap (MOT). The atomic cloud is overlapped with a far-off resonance dipole trap at the 813 nm magic wavelength of the $^1S_0$ - $^3P_0$ clock transition. At this wavelength the differential ac-Stark shift of the second stage cooling transition is nearly zero and allows simultaneous Doppler cooling in the FORT [10].

II. Doppler cooling of ^{88}Sr

Figure 1 shows a simplified level scheme for atomic strontium. Doppler cooling of strontium is done in two steps. In the first cooling process, atoms are cooled down to the millikelvin regime on the broad $^1S_0$ - $^1P_1$ transition at 461 nm using a standard six-beam magneto-optical trap (MOT). This transition shows a linewidth of $\gamma/2\pi = 32$ MHz with a saturation intensity of 43 mW/cm^2. The effective loss rate per $^1P_1$ atom along the $^1D_2$ - $^3P_2$ decay path is around $1.3 \times 10^3\ s^{-1}$ which is a factor of 160,000 times smaller than the cooling transition rate of $\Gamma = 2.1 \times 10^8\ s^{-1}$. To eliminate the $^3P_2$ shelving loss two repumping lasers at the $^3P_0$ - $^3S_1$ and $^3P_2$ - $^3S_1$ transitions are needed [11], but in contrast to all alkali-atom MOTs, where repumping is essential, the 461 nm strontium MOT can be established without repumping lasers.

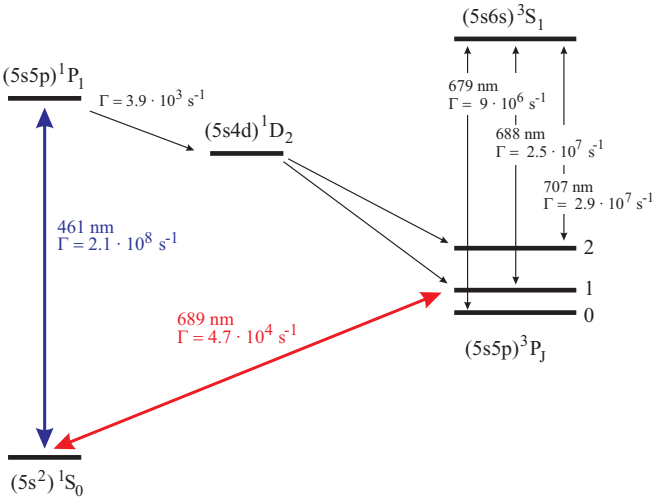

Fig. 1. Simplified electronic level structure of atomic strontium showing the cooling transitions at 461 nm and 689 nm as well as the radiative decay channel for the $^1P_1$ excited state. Repumping during the 461 nm cooling is possible (but not mandatory) via the $^3S_1$ state. Γ denotes the transition Einstein A coefficient.

The spin-forbidden $^1S_0$ - $^3P_1$ transition at 689 nm with a linewidth of $\gamma/2\pi = 7.6$ kHz and a saturation intensity of $I_{sat} = 3$ μW/cm^2 is used in the second cooling step. Its line width is even smaller than the Doppler shift caused by a single photon recoil, i.e. $\Delta\omega/2\pi = \hbar k^2/2\pi m = 9.6$ kHz. The reabsorption of spontaneous emitted photons during laser cooling is minimized and magneto-optically trapped strontium atoms at the recoil temperature with a phase space density of 10^{-2} has been demonstrated by Katori et al. [12]. To cover the Doppler shift of the atoms from the first cooling stage and to compensate for the limited velocity capture range of the 689 nm MOT, the frequency of the red cooling laser was broadened to 1.5 MHz.

We follow this technique and use a two stage MOT to cool

1-4244-0647-1/07/$20.00 ©2007 IEEE

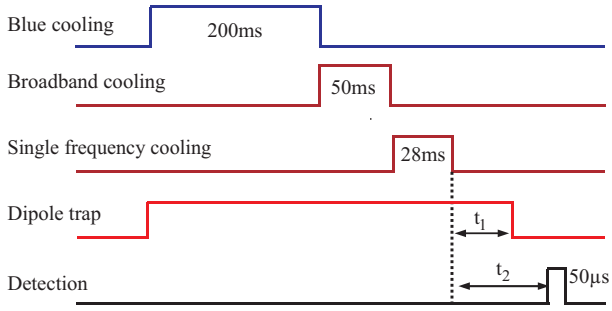

Fig. 2. Sequence of the experiment. The first cooling stage (blue cooling) operates at the $^1S_0$ - $^1P_1$ transition at 461 nm. The broadband and the single-frequency cooling stages utilizes the narrow intercombination line at 689 nm. For loading atoms into the FORT, the dipole laser beam at 813 nm is switched on simultaneously with the 461 nm cooling laser. In order to measure temperature and atom number, the shadow of the atomic cloud is imaged on a CCD camera by a 50 μs long laser pulse near resonant to the 461 nm transition.

the atoms down to the microkelvin regime. Initially the atoms were decelerated to a velocity of 30 m/s by a 30 cm long Zeeman-slower. To avoid the light pressure from the slowing beam at 461 nm and collisions with hot atoms we use a two-dimensional optical molasses at the end of the slower to deflect the slow atoms towards the center of the MOT.

About 200 mW of 461 nm radiation for the first cooling stage is generated by the frequency-doubled infrared radiation of a Ti:sapphire laser. For frequency-doubling we use a periodically poled KTP crystal in a bow tie ring cavity. For short term frequency stability, the Ti:sapphire laser is locked to a reference cavity and for the long term stability to an auxiliary strontium atomic beam.

The 689 nm laser for second-stage cooling is an extended-cavity master diode laser and an injection locked slave laser. To provide sufficient frequency stability the master laser is locked to a reference cavity by the Pound-Drever-Hall method [13]. The non-tunable reference cavity made from Zerodur is mounted in a temperature stabilized vacuum chamber. The frequency offset between the cavity resonance and the atomic frequency is bridged with an acousto-optical modulator (AOM). The spectrum for the broadband cooling on the narrow transition is broadened by an AOM, that operates from a frequency modulated rf-source.

The time sequence of the two-stage MOT is shown in Figure 2. The blue cooling stage lasts for 200 ms. During this time, the MOT is loaded from the Zeeman-slowed atomic beam. The magnetic field gradient is 17 mT/cm. The MOT beams have a $1/e^2$ diameter of 10 mm and total intensity of 16 mW/cm^2. The laser is detuned 40 MHz below the $^1S_0$ - $^1P_1$ transition frequency. This process ends up in 3×10^7 atoms at a temperature of 2 mK. All 461 nm laser beams are switched off and the precooled atoms are transferred into the second stage MOT at the 689 nm transition. For the broadband cooling, the laser frequency is tuned 1.6 MHz below the $^1S_0$ - $^3P_1$ transition and sinusoidally modulated at 50 kHz with a maximum frequency shift of 1.5 MHz. The optimum magnetic field gradient for the 689 nm MOT is around 0.5 mT/cm

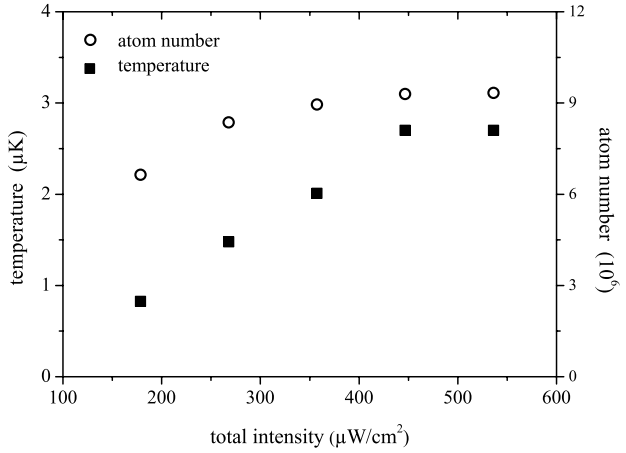

Fig. 3. Change of atomic-cloud temperature and number of atoms as a function of the total laser intensity of the single-frequency cooling stage. In each measurement the initial number of atoms in the 461 nm MOT was around 3×10^7. The saturation intensity of the 689 nm transition is 3 μW/cm^2.

and the optimal laser intensity is 8 mW/cm^2. Within the 50 ms long broadband cooling the atoms were cooled down to 15 μK. In the end the frequency modulation is switched off and the cooling lasers operate at a single frequency detuned 400 kHz below the $^1S_0$ - $^3P_1$ transition with an intensity of 550 μW/cm^2. After 28 ms we find 7×10^6 atoms at a temperature of around 2.5 μK. The overall loading efficiency from the 461 nm MOT to this stage is around 23 %. We determine the atomic-cloud temperature from the thermal expansion of the atomic cloud after turning off the MOT. In a sequence of loading and release experiments varying the expanding time the shadow of the atomic cloud is imaged on a CCD camera. The imaging 50 μs long laser pulse is near resonant to $^1S_0$ - $^1P_1$. From the absorption image we determine also the optical density of the atom cloud which allows us to calculate the atom number N.

To achieve even lower temperatures, the cooling laser intensity of the last cooling stage can be reduced. Figure 3 shows the temperature of the atomic cloud as well as the atom number in the 689 nm MOT in dependance of the cooling laser intensity. Due to reduced saturation of the cooling transition the temperature is decreased down to 0.8 μK. The reduced power broadening leads to a slight decrease in the number of atoms.

III. Far-off resonance dipole trap

As a first step towards ultracold strontium atoms confined in an optical lattice, we investigate the loading of ^{88}Sr from the MOT at 689 nm into a far-off resonance dipole trap at a wavelength of 813 nm. The dipole trapping laser is 340 nm detuned from the $^1S_0$ - $^1P_1$ transition. For a dipole laser intensity of 42 kW/cm^2 the photon scattering is below 1 s^{-1}, which is negligible for most practical purposes.

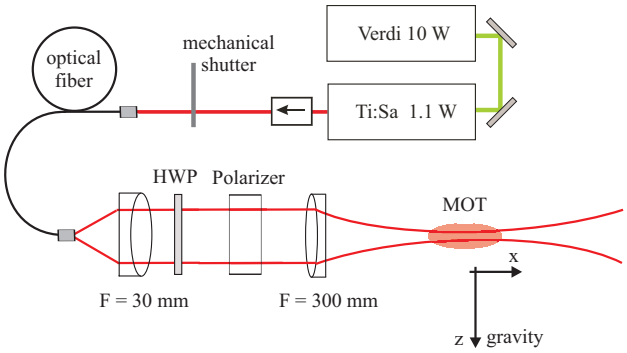

Fig. 4. Setup of the 1-D far-off resonance dipole trap at 813 nm. The radiation from the polarization maintaining single-mode fibre is focused onto the ultracold atomic cloud. The beam waist radius of the dipole trap is 30 μm. With dipole trap beam power of up to 600 mW, an effective trap depth of up to 24 μK is realized. The dipole trap is directed perpendicular to gravity and to the axis of the MOT coils.

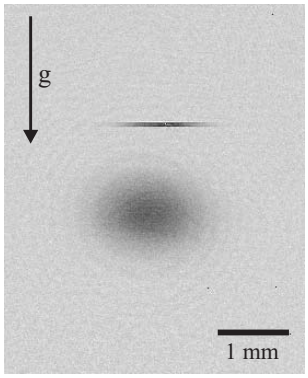

Fig. 5. Absorption image of strontium atoms trapped in the 1-D FORT. Also visible is the expanded atomic cloud of untrapped atoms 14 ms after the 689 nm MOT has been turned off. The temperature of the untrapped atomic cloud is determined to 4 μK. Gravity is directed downwards.

In most dipole trapping experiments the ac-Stark shifts do not allow a simultaneous Doppler cooling during dipole trap loading. However, in alkaline earth elements, like strontium, the intercombination line enables a light-shift cancelation technique. The dipole trap laser couples the singlet and the triplet states independently which results in different dependencies of the light shift of the $^1S_0$ and the $^3P_1$ state. At the so called "magic wavelength" the differential shifts of the 689 nm cooling transition vanishes and the detuning of the cooling transition is no longer position-dependent. Therefore Doppler cooling in the dipole trap is possible. Katori et al. have shown, that the magic wavelength of the strontium $^1S_0$ - $^3P_1$ intercombination line is about 800 nm [10], [14]. We investigate Doppler cooling of strontium into a FORT at the 813 nm magic wavelength of the $^1S_0$ - $^3P_0$ clock transition, which is near to the magic wavelength of the cooling transition at 689 nm.

The FORT potential of a dipole trap beam oriented perpendicular to gravity g, according to Figure 4, is given by

$$U(y,z) = -U_0 \exp(-(y^2+z^2)/w_0^2) + mgz. \qquad (1)$$

Here w_0 indicates the beam waist radius, mgz is the gravitational potential of the atoms with mass m and U_0 is the maximum Stark shift potential. The trap potential along the z-direction is shown in the inset of Figure 6. The effective potential depth ΔU describes the lowest potential barrier against gravity and atoms with energy $E > \Delta U$ cannot be trapped.

The setup of the dipole trap optics is shown in Figure 4. As a dipole trap laser we use a Ti:sapphire laser with 1.1 W output power at 813 nm. Its output beam is coupled into a polarization-maintaining optical fiber and can be blocked by a galvo-scanner driven mechanical shutter. The 670 mW output beam at the optical fiber output passes through polarization optics before being focused on the center of the atomic cloud. The horizontally directed trap beam is linearly polarized with its polarization oriented perpendicular to axis of the magnetic coils of the MOT. With a beam waist radius of 30 μm and a power of 600 mW a maximum intensity of 42 kW/cm^2 is realized. This corresponds to a maximum Stark shift potential of $U_0 = 30$ μK whereas the effective potential depth is $\Delta U = 24$ μK.

Figure 2 includes the loading sequence into the FORT. The dipole trap is operated simultaneously with the two stage Doppler cooling. In order to get an absorption image of the trapped atoms, the 689 nm MOT is turned off while the dipole trap laser remains on. Due to gravity all atoms not confined in the FORT are separated from the dipole-trapped atoms. Figure 5 shows the absorption image of the trapped atoms as well as the free falling atomic cloud $t_2 = 14$ ms after the MOT has been switched off. The absorption image is done using a 50 μs long detection pulse near resonant to $^1S_0$ - $^1P_1$ transition.

Since the absorption image of the dipole trapped atoms on the CCD camera is only a few pixels in height and the absorption is saturated, no reliable atom number determination as explained above is possible during dipole trap operation. In order to measure the atom number in the FORT, the dipole trap laser has been blocked by the mechanical shutter $t_1 = 12$ ms after releasing the atomic cloud. After time $t_2 = 14$ ms we use the 50 μs long detection pulse to get the absorption image of the expanded atomic cloud. Figure 6 shows the number of trapped atoms in the FORT in dependence of the effective trap potential ΔU. For each measured point, the total intensity of the MOT beams at 689 nm has been chosen to be 540 μW/cm^2 resulting in 9×10^6 atoms at a temperature of about 3 μK. At an effective trap depth of 8 μK roughly 10 % of the atoms have been transferred from the MOT into the dipole trap. With increasing potential depth, the number of trapped atoms is increasing until it saturates at an effective trap depth of around 20 μK. At this value a transfer efficiency of 60 % has been reached resulting in 5.5×10^6 trapped atoms.

IV. Conclusion

We have cooled strontium atoms in a two stage MOT to temperatures below 1 μK using the spin forbidden $^1S_0$ - $^3P_1$

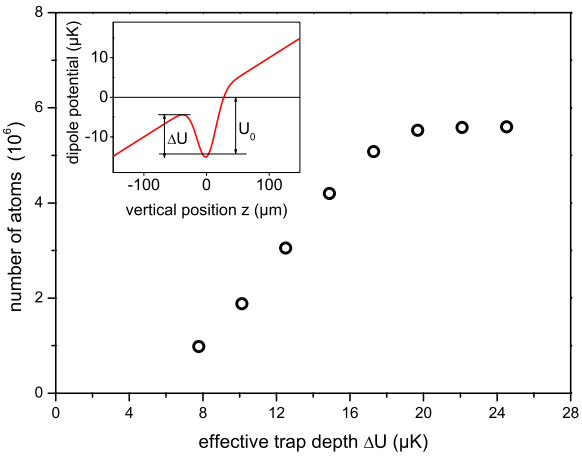

Fig. 6. Number of dipole trapped atoms as a function of the effective trap potential. The inset shows the trap potential along gravity. U_0 indicates the maximum Stark shift due to the dipole trapping laser whereas ΔU is the potential barrier holding the atoms against gravity.

transition. The second cooling stage at 689 nm is compatible with loading atoms in a 1-D far-off resonance dipole trap. The simultaneous operation of the MOT and the FORT enables a transfer efficiency into the dipole trap of around 60%. This set-up will be extended to load and confine atoms into a 1-D optical lattice, which is an important prerequisite for investigating an optical lattice clock using the magnetically induced $^1S_0$ - $^3P_0$ transition in ^{88}Sr.

ACKNOWLEDGMENT

The authors gratefully acknowledge the support by the Deutsche Forschungsgemeinschaft under SFB 407.

REFERENCES

[1] M. Takamoto, F.-L. Hong, R. Higashi, and H. Katori, "An optical lattice clock," *Nature*, vol. 435, pp. 321–324, 2005.

[2] R. Le Targat, X. Baillard, M. Fouché, A. Brusch, O. Tcherbakoff, G. D. Rovera, and P. Lemonde, "Accurate optical lattice clock with ^{87}Sr atoms," *Phys. Rev. Lett.*, vol. 97, pp. 130 801–1–4, 2006.

[3] M. Takamoto, F.-L. Hong, R. Higashi, Y. Fujii, M. Imae, and H. Katori, "Improved frequency measurement of a one-dimensional optical lattice clock with a spin-polarized fermionic ^{87}Sr isotope," *J. Phys. Soc. Jap.*, vol. 75, pp. 104 302–1–10, 2006.

[4] A. D. Ludlow, M. M. Boyd, T. Zelevinsky, S. M. Foreman, S. Blatt, M. Notcutt, T. Ido, and J. Ye, "Systematic study of the ^{87}Sr clock transition in an optical lattice," *Phys. Rev. Lett.*, vol. 96, p. 033003, 2006.

[5] M. M. Boyd, A. D. Ludlow, S. Blatt, S. M. Foreman, T. Ido, T. Zelevinsky, and J. Ye, "^{87}Sr lattice clock with inaccuracy below 10^{-15}," *Phys. Rev. Lett.*, vol. 98, p. 083002, 2007.

[6] R. Santra, E. Arimondo, T. Ido, C. H. Greene, and J. Ye, "High-accuracy optical clock via three-level coherence in neutral bosonic ^{88}Sr," *Phys. Rev. Lett.*, vol. 94, pp. 173 002–1–4, 2005.

[7] T. Hong, C. Cramer, W. Nagourney, and E. N. Fortson, "Optical clocks based on ultranarrow three-photon resonances in alkaline earth atoms," *Phys. Rev. Lett.*, vol. 94, p. 050801, 2005.

[8] A. V. Taichenachev, V. I. Yudin, C. W. Oates, C. W. Hoyt, Z. W. Barber, and L. Hollberg, "Magnetic field-induced spectroscopy of forbidden optical transitions with application to lattice-based optical atomic clocks," *Phys. Rev. Lett.*, vol. 96, p. 083001, 2006.

[9] X. Baillard, M. Fouché, R. L. Targat, P. G. Westergaard, A. Lecallier, Y. L. Coq, G. D. Rovera, S. Bize, and P. Lemonde, "Accuracy evaluation of an optical lattice clock with bosonic atoms," arXiv:physics/0703148v1, 2007.

[10] H. Katori, T. Ido, and M. Kuwata-Gonokami, "Optimal design of dipole potentials for efficient loading of Sr atoms," *J. Phys. Soc. Jap.*, vol. 68, pp. 2479–2482, 1999.

[11] X. Xu, T. H. Loftus, J. L. Hall, A. Gallagher, and J. Ye, "Cooling and trapping of atomic strontium," *J. Opt. Soc. Am. B*, vol. 20, pp. 968–976, 2003.

[12] H. Katori, T. Ido, Y. Isoya, and M. Kuwata-Gonokami, "Magneto-optical trapping and cooling of strontium atoms down to the photon recoil temperature," *Phys. Rev. Lett.*, vol. 82, pp. 1116–1119, 1999.

[13] R. W. P. Drever, J. L. Hall, F. V. Kowalski, J. Hough, G. M. Ford, A. J. Munley, and H. Ward, "Laser phase and frequency stabilization using an optical resonator," *Appl. Phys. B*, vol. 31, pp. 97–105, 1983.

[14] T. Ido, Y. Isoya, and H. Katori, "Optical-dipole trapping of Sr atoms at a high phase-space density," *Phys. Rev. A*, vol. 61, pp. 061 403–1–4, 2000.